Available online at www.elixirpublishers.com (Elixir International Journal)

Vibrational Spectroscopy

Elixir Vib. Spec. 151A (2021) 55242-55249

ISSN: 2229-712X

Quantum Ab-Initio Study, Thermodynamic Analysis and Frontier Molecular Orbital of Exalite-392A

Alande Balaji D[1], Sushma G.N.[2], Y.F. Nadaf[2,*] and Basavaraja Sannakki[1,*]

[1]Dept. of Physics, Jnana Ganga Campus, Gulbarga University, Kalaburgi - 585106, India.

[2]Dept. of Physics, Materials Research Centre, Maharani Science College for Women, Maharani Cluster University, Bengaluru-560001, India.

ARTICLE INFO

Article history:

Received: 11 January 2021;

Received in revised form:

10 February 2021;

Accepted: 20 February 2021;

Keywords

UV-Vis,

FMO,

Mulliken Charge,

E-392A, MEP.

ABSTRACT

In this article computational study by using DFT on Exalite–392A is reported. The quantum mechanical analysis of various energies of molecule in ground state was calculated by using DFT technique. The effect of the solvent on optimized geometry, Mulliken charge distribution in ground and excited state were analysed. With the help of computed highest occupied molecular orbital (HOMO) - lowest unoccupied molecular orbital (LUMO) gap of Exalite–392A in different medium, we can analysed solvation energy, ionization potential, electron affinity, chemical hardness, electron chemical potential, electronegativity and global electrophilic. UV-Vis spectrum was obtained by using TDDFT technique. The total electron density (TED), potential distribution over molecule by electrostatic potential (ESP) positions of molecule were obtained from molecular electrostatic potential (MEP) and frontier molecular orbitals (FMO) simulated. Main objective is to determine their electronic, thermodynamic and spectroscopic parameters on the basis of the DFT quantum chemical studies and also we are studying the effect of solvent and solute-solvent interactions. This molecule is helpful in designing of laser materials.

1. Introduction

The exalite laser grade dye series are identified as unique popular dye laser fields and impacted significant attention in applied fields starting from molecular spectroscopy to dermatology. The exalite dye molecules have found applications in many areas of research. When pumped by XeCl-excimer [1–3], Ar [4] and Nd: YAG [5–7] lasers this dye provide tunable lasers in the ultraviolet–blue range [8].

From the literature survey, no theoretical studies have been found for Exalite–392A. We are carried out a theoretical study using Density Functional Theory (DFT) and Time-Dependent Density Functional Theory (TD-DFT)for the Exalite–392A, which were treated according to Becke's three Lee–Yang– Parr (B3LYP) gradient correlation potential and all evaluation were finished with the aid of basis set 6-311G [9-11]. DFT and TDDFT are used to analyze the optical parameters of each organic and inorganic molecules, DFT is implemented for studying the ground state (GS) parameters of molecule and TD-DFT used for modeling the energies, systems and properties of electronically excited states (ES), DFT presents the theoretical prediction of molecule useful in drug designing and allows us to understanding the chemical methods in organic structures [12].

Therefore, the systematic investigation of geometrical properties, thermodynamic properties, structural properties, frontier molecular orbital analysis, total electron density (TED), electrostatic potential (ESP), molecular electrostatic potential (MEP) of Exalite–392A with the help of quantum chemical analysis [13, 14]. Furthermore, absorption study was performed with TDDFT in order to explain differences due to liquid and gas phase.

2. Computational details

The simulation studies on Exalite–392A have been carried out by building its structure using Gauss view 5.0 and Gaussian 09 W software package is used for all theoretical studies included in the article. Initially the geometry became optimized by means of DFT with B3LYP functional and 6-311G basis set, the atomic charge distribution in the ground state and TDDFT in the excited state [15], thermodynamic properties, structural properties and optical properties were studied the use of DFT method B3LYP/6-311G and frontier molecular orbital (FMO) analysis of molecule in vacuum and ethanol were studied.

The thermodynamical parameters, SCF energy, enthalpy, entropy, dipole moment, zero-point vibrational energy, heat capacity, and rotational constants are calculated. UV-Vis and emission spectroscopic studies have done for Exalite–392A computed in different medium and recorded the energy maximum with oscillatory strength using TDDFT method with B3LYP /6-311G level of study. The energy values in different molecular orbitals of HOMO and LUMO is noted in different medium and the energy separation between these molecular orbital is prolonged to analyze various molecular factors like ionization ability, electron chemical capacity, electronegativity, electron affinity, chemical hardness, and international electrophilic index and so on., TED surface mapping, ESP, MEP and contour mapping of the molecule in vacuum and solvent medium is determined using DFT method. Therefore, in this present work, our primary aim is to

Tele:

E-mail address: dryfnadaf@gmail.com, sannakk.phy@gmail.com,

compute complete theoretical studies on the Exalite – 392A molecule [16].

3. Results and Discussion

3.1 Structure and geometric properties

The structure of Exalite–392A from the gauss view is geometrically optimized by using Gaussian 09 with keyword opt, B3LYP functional and 6-311G basis set [17]. Initial geometry obtained from standard parameters which are then reduced to a minimum by the Gaussian program which computes the energies to discover the molecular geometry similar to the minimum energy. The optimized geometries of Exalite–392A are illustrated in Figure 1 [18]. The ground and excited geometries of the molecule was studied by using DFT/B3LYP/6-311G and TDDFT/B3LYP/6-311G level respectively. The geometrical properties have been given in Table 1, there is no significant changes in molecular geometry of 9Cl1,2Dm10MsQ from ground state to excited state, so we observe the similarities in bond length (Å), bond angle (º) and dihedral angle (º) in both the states [19].

3.2 Mulliken atomic charge distribution

The distribution of Mulliken atomic charge on each atomic site of Exalite-392A was analysed using DFT/B3LYP/6-311G in vacuum medium and ethanol solvents. Distribution of Mulliken charge on each atom of Exalite-392A was presented in Table 2 and charge distribution in different medium is represented as shown in Figure 2. The solvent influences on the atomic charges are observed from the analysis. The values of atomic charges in ethanol are higher variation than in vacuum. The carbon atoms which have the positive charge acts as acceptor and the carbon atoms with negative charge acts as donator and all hydrogen atoms acts as an acceptor [20].

3.3 Thermodynamic parameters

The useful chemical processes can be identified with the help of thermodynamic parameters. DFT simulations are helpful for studying statistical thermodynamic properties of the compound. Translational energy, rotational energy, vibrational energy, total energy, nuclear repulsion energy, zero-point vibrational energy and the statistical thermodynamic properties, such as, entropy (S), rotational constants, rotational temperatures, molecular capacity of constant volume, dipole moment were obtained from the theoretical harmonic frequencies calculated by DFT/B3LYP/6-311G level of theory for the Exalite-392A molecule at room temperature and 1 atm pressure and given in Table 3. These calculated thermodynamic parameters are helps for further systematic understanding of molecule [21].

3.4 Spectroscopic study

By using TDDFT the excited states of Exalite-392A in vacuum and ethanol medium are analysed and presented in Table 4. The TDDFT studies are helps to examine the absorption spectra that have been furnished an effective approach [22, 24], and the highest wavelength at 338.85nm with an oscillator strength f = 1.7481in vacuum as presented in Figure 3.

3.5 Frontier Molecular Orbitals and Quantum chemical calculation

With the help of FMO the electron charge transfer between the donor and acceptor group can be determined. The HOMO (electron-donating) directly associated with the ionization potential, even as the LUMO (electron-accepting) associated with the electron affinity of the compound. FMO used to have higher information of the nature of the chemical structure and chemical reaction of the molecule [25]. HOMO, HOMO-1, HOMO-2 are the orbitals that Present π-bonding symmetry and LUMO, LUMO+1, LUMO+2 are molecular orbitals that shows π* antibonding symmetry represented in Table 5. Figure 4 shows the 3D representation of frontier molecular orbital in different medium using method with B3LYP functional and 6-311G basis set in which greenish area represents the positive region and reddish area shows the negative region of the molecular orbital.

Energy gap (E_g) has been analysed using the equation, which gives energy gap (E_g) between HOMO to LUMO. The E_g in vacuum medium indicate the higher value energy gap of 4.1263 eV [26]. By DFT theory of quantum chemical factors, negative of HOMO energy is taken as ionization potential (I) and negative of LUMO energy as electron affinity (E) can be obtained. I and E are important features of organic molecules and ions, which makes it possible to get the molecular reactivity and interpret the results of electronic spectra. The E_g I and E values are helps us to analyze the various parameters like chemical hardness (η), chemical potential (μ), chemical softness (s), global electrophilicity(ω) of the Exalite–392A molecule in vacuum and solvent medium as shown in Table 6 [27].

The energy band gap $(\mathbf{Eg} = \boldsymbol{E_{HOMO} \sim E_{LUMO}})$ can be obtained from HOMO and LUMO, the ability of atoms to attract the shared electrons of covalent bond gives electronegativity $(\mathbf{x} = (\mathbf{I} + \mathbf{E})/\mathbf{2})$ chemical hardness $\eta(= (\mathbf{I} - \mathbf{E})/\mathbf{2})$ is half of the energy band gap , the chemical potential is obtained by the negative value of electronegativity $(\boldsymbol{\mu} = -\boldsymbol{\chi})$, and chemical softness $(\mathbf{S} = {}^{\mathbf{1}}/_{\mathbf{2\eta}})$ Therefore global electrophilicity $(\omega = \mu^{\mathbf{2}}/\mathbf{2}\eta)$ can be calculated [28].

3.6 ESP, TED and MEP studies.

Using the DFT theory with B3LYP/6-311G model ESP, TED and MEP maps are obtained, and the 3D geometrical presentation are given in Figure 5.

3.6.1 Total Electron Density (TED)

To analysis shape, charge, size, delocalization of molecule and location of chemical reactivity of the molecule the TED studies are essential, TED plots are shown in Figure. 5. (a), which indicates the uniform distribution [29] for the Exalite–392A molecule in vacuum and solvent medium.

3.6.2 Electrostatic Potential (ESP)

For better understanding of intermolecular association, molecular properties of the compound ESP study was used and also it provides information about location of electrophilic and nucliophilic siter. By the ESP study, the energy of Exalite–392A ranges in vacuum medium is between -0.0937 eV to 0.0937 eV and in ethanol from -0.2889 eV to 0.2889 eV are found. We absorved red color at the site of carbon atoms in benzene ring and surrounded by yellow colour in Figure 5(b).

3.6.3 Molecular Electrostatic Potential (MEP)

The MEP studies are useful for understanding the molecular parameters, charge density, and polarity of the compound. Red colour represents the maximum negative potential region, the blue colour represents the maximum positive potential region and green represents the zero potential areas [30]. Figure 5(c) represents the 3D MEP mapping of the compound in vacuum and solvents. In different medium the MEP shows almost same mapping surfaces with similar type of colour code. Inside benzene rings are nucliophilic attack regions because of its maximum negative potential due to mesmeric effect with large electronic charge indicates reddish colour. The hydrogen atoms represents large positive potential surface and results to

an electrophilic attack region with a blue shade surrounding, the greenish shade of the molecule shows the zero potential.

4. Conclusions

The computational studies using DFT and TDDFT methods to the Exalite-392A molecule were carried out by consideration of the geometrical and structural properties that, a few precise distances and angles can impact the orbital overlap and HOMO-LUMO energy distribution. The UV-Visible absorption properties were acquired primarily based on TD-DFT calculations. The FMO energy gap helpful for represent the high chemical reactivity and stability of the molecule. A compound with a less E_g is commonly related to an excessive chemical reactivity, low kinetic stability and is also known as soft molecule. These theoretical studies helps in better understanding of Exalite-392A which can be used as, biomedical inhibitor, fluorescent tag and a laser dye in other applied applications.

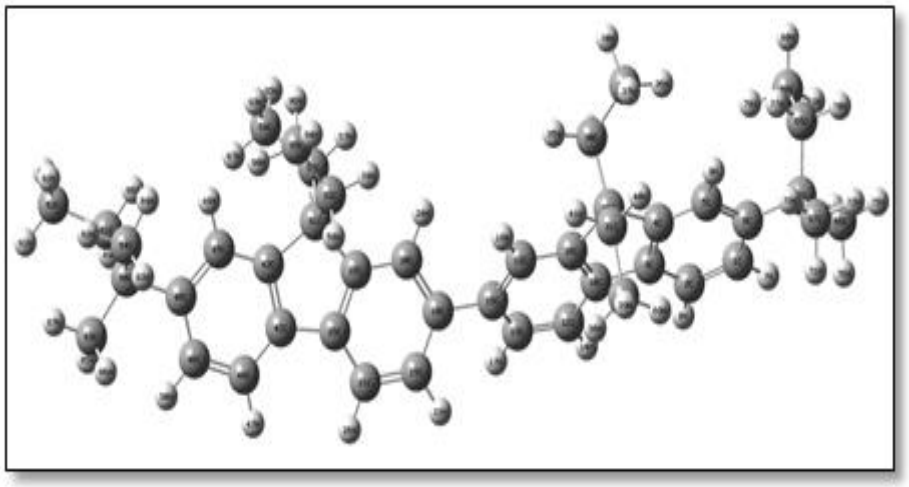

Figure 1. Optimized molecular Structure of Exalite-392A

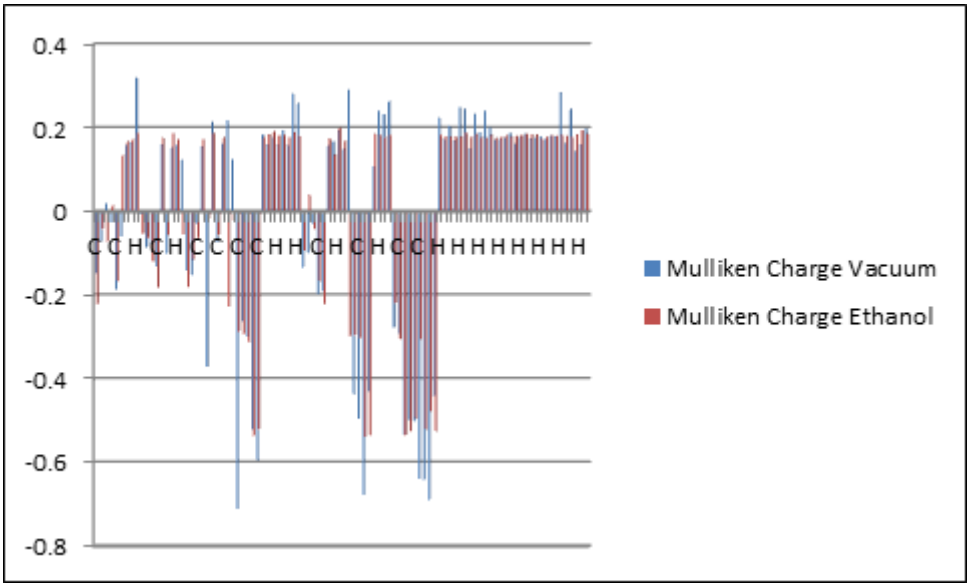

Figure 2. Mulliken atomic charge distribution of Exalite-392A in vacuum and ethanol medium using DFT method

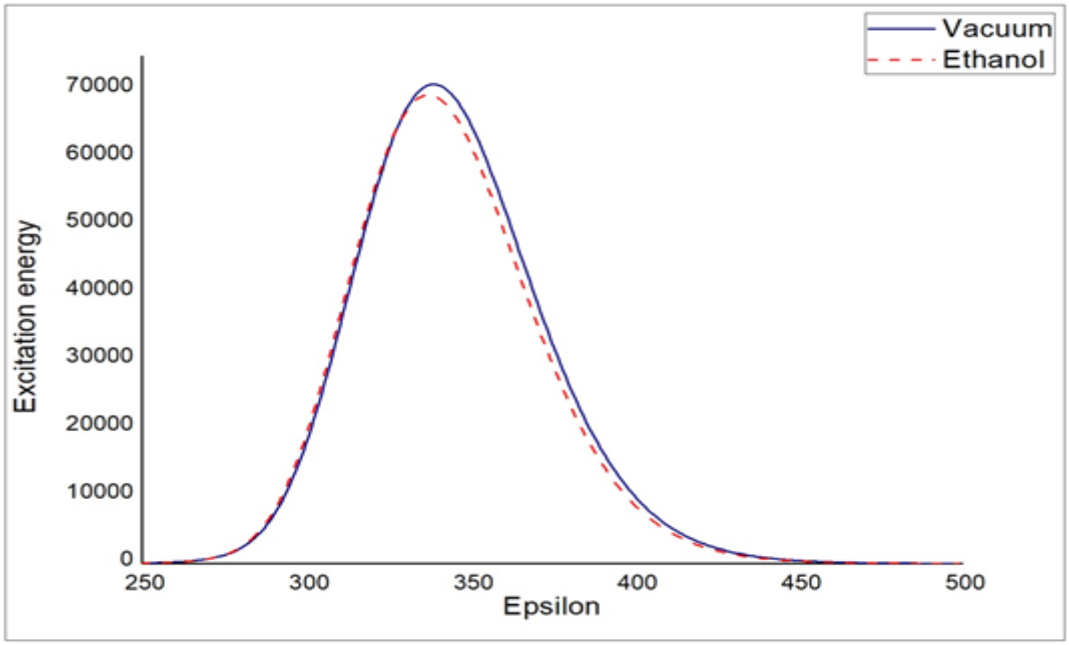

Figure 3. Absorption spectra of Exalite -392A in vacuum and solvent medium using TDDFT analysis

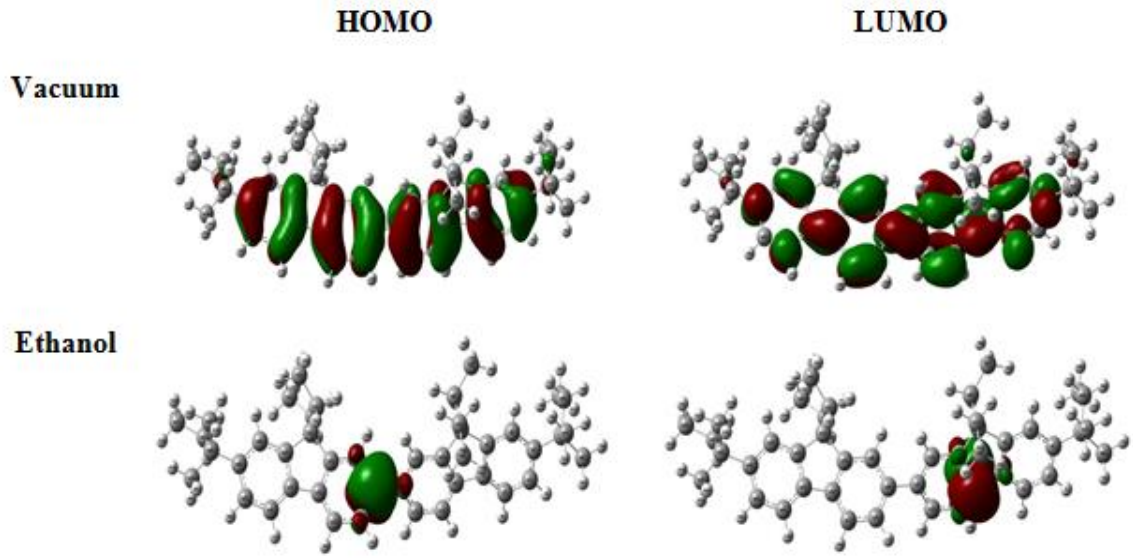

Figure 4. 3D representations of HOMO and LUMO in vacuum and ethanol medium using DFT method

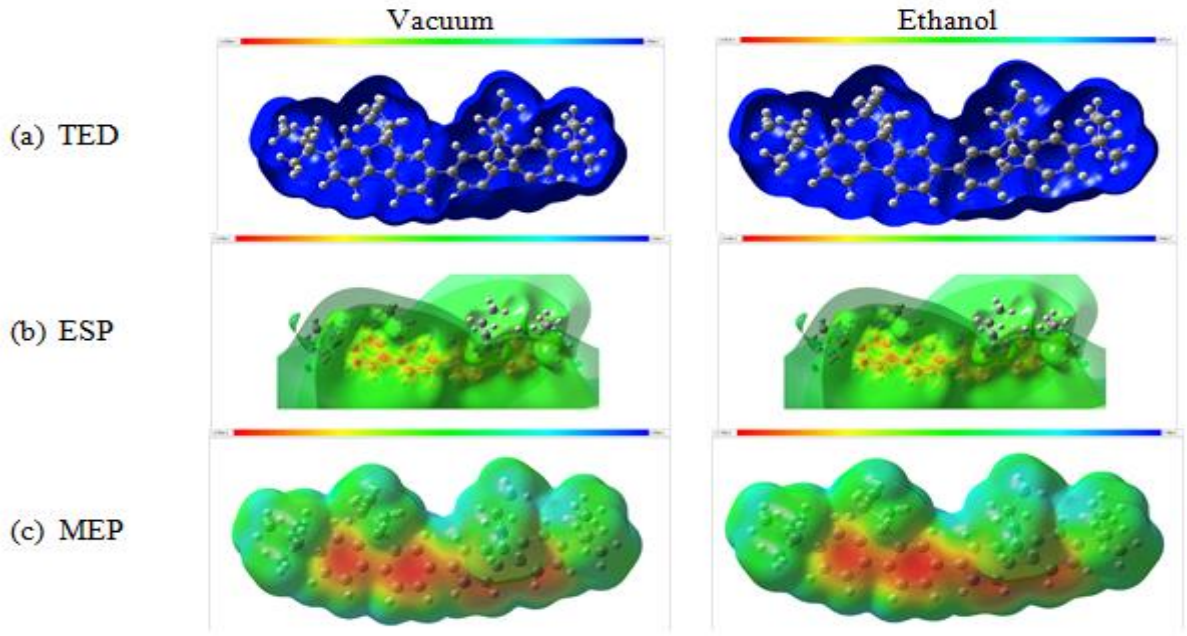

Figure 5(a) TED mapping, (b) ESP and (c) MEP surface of Exalite -392A in vacuum and ethanol medium

Table 1. Bond length (Å), bond angle (º) and dihedral angle (º) of Exalite – 392A using DFT/B3LYP/6-311G and TDDFT/ B3LYP/6-311G

Atoms	Bond length (Å)		Atoms	Bond Angle (º)		Atoms	Dihedral Angle (º)	
	Ground State	Excited state		Ground State	Excited state		Ground State	Excited state
2C-1C	1.399838	1.399837	3C-2C-1C	119.4278	119.4278	4C-3C-2C-1C	0.506431	0.502021
3C-2C	1.392893	1.392899	4C-3C-2C	119.9352	119.9349	5C-4C-3C-2C	-1.58376	-1.58182
4C-3C	1.414019	1.41402	5C-4C-3C	119.9833	119.9836	6C-1C-2C-3C	0.614079	0.619505
5C-4C	1.389453	1.389445	6C-1C-2C	121.7523	121.7516	7H-1C-2C-3C	-179.968	-179.961
6C-1C	1.40455	1.404538	7H-1C-2C	118.2638	118.2646	8H-2C-1C-6C	-178.907	-178.91
7H-1C	1.079534	1.079537	8H-2C-1C	119.6626	119.6627	9H-5C-4C-3C	-177.811	-177.807
8H-2C	1.082871	1.082874	9H-5C-4C	119.7241	119.7244	10C-3C-2C-1C	-177.658	-177.665
9H-5C	1.081083	1.081089	10C-3C-2C	131.2479	131.2482	11C-10C-3C-2C	-0.61761	-0.61574
10C-3C	1.46694	1.466935	11C-10C-3C	131.3906	131.3913	12C-10C-3C-2C	177.6775	177.6803
11C-10C	1.396657	1.396653	12C-10C-3C	138.0943	138.0937	13C-11C-10C-3C	178.7629	178.762
12C-10C	2.429824	2.429829	13C-11C-10C	119.2664	119.2666	14H-11C-10C-3C	-1.65724	-1.65835
13C-11C	1.39564	1.395643	14H-11C-10C	120.891	120.8915	15C-13C-11C-10C	-0.04236	-0.03888
14H-11C	1.082651	1.082652	15C-13C-11C	121.5126	121.5129	16H-12C-10C-3C	-1.78263	-1.78118
15C-13C	1.409783	1.409782	16H-12C-10C	150.4971	150.4972	17H-13C-11C-10C	178.4209	178.4195
16H-12C	1.082647	1.082648	17H-13C-11C	119.3631	119.3622	18C-15C-13C-11C	-179.793	-179.798
17H-13C	1.081716	1.081716	18C-15C-13C	120.7376	120.7391	19C-18C-15C-13C	39.03924	39.03197
18C-15C	1.48576	1.485759	19C-18C-15C	120.7595	120.761	20C-18C-15C-13C	-140.959	-140.968
19C-18C	1.409648	1.409643	20C-18C-15C	120.7394	120.7385	21C-19C-18C-15C	-179.842	-179.839
20C-18C	1.41197	1.411965	21C-19C-18C	121.4702	121.4707	22H-19C-18C-15C	1.799153	1.801181
21C-19C	1.395458	1.395454	22H-19C-18C	119.1334	119.1331	23C-20C-18C-15C	179.8749	179.8705
22H-19C	1.081696	1.081697	23C-20C-18C	120.2612	120.2617	24H-20C-18C-15C	1.673351	1.683264
23C-20C	1.38882	1.388823	24H-20C-18C	119.155	119.1586	25C-21C-19C-18C	-0.04536	-0.04741
24H-20C	1.082389	1.082385	25C-21C-19C	119.2719	119.2726	26H-21C-19C-18C	-179.513	-179.512
25C-21C	1.396773	1.396773	26H-21C-19C	119.8371	119.8362	27C-6C-1C-2C	178.9736	178.9689
26H-21C	1.082633	1.082634	27C-6C-1C-2C	122.6712	122.6703	28C-12C-10C-3C	1.361005	1.360096
27C-6C	1.544131	1.544149	28C-12C-10C	30.02603	30.02611	29C-28C-12C-10C	178.9456	178.9442
28C-12C	1.3884	1.388393	29C-28C-12C	128.5996	128.5993	30C-29C-28C-12C	-64.0632	-64.0636
29C-28C	1.537158	1.537161	30C-29C-28C	107.5669	107.5665	31C-29C-28C-12C	57.99792	57.99876
30C-29C	1.569087	1.569096	31C-29C-28C	112.3736	112.3745	32C-30C-29C-28C	-177.009	-177.007
31C-29C	1.556204	1.556189	32C-30C-29C	117.4544	117.4544	33C-31C-29C-28C	54.58302	54.58005
32C-30C	1.535467	1.535466	33C-31C-29C	115.1117	115.1142	34H-30C-29C-28C	-53.5073	-53.5055
33C-31C	1.53522	1.53522	34H-30C-29C	107.5461	107.5452	35H-30C-29C-28C	60.28906	60.29088
34H-30C	1.093177	1.093177	35H-30C-29C	106.9714	106.9715	36H-32C-30C-29C	63.9061	63.90347
35H-30C	1.094773	1.094772	36H-32C-30C	111.7791	111.7798	37H-32C-30C-29C	-58.1045	-58.1074
36H-32C	1.090122	1.090125	37H-32C-30C	112.3361	112.3359	38H-33C-31C-29C	-60.7809	-60.7811
37H-32C	1.091328	1.09133	38H-33C-31C	111.4242	111.4241	39H-33C-31C-29C	179.3975	179.3966
38H-33C	1.090643	1.090644	39H-33C-31C	110.4038	110.4042	40H-31C-29C-28C	177.1509	177.1488
39H-33C	1.092218	1.092219	40H-31C-29C	108.5644	108.564	41H-31C-29C-28C	-68.1086	-68.1112
40H-31C	1.093289	1.093295	41H-31C-29C	108.0041	108.0025	42C-25C-21C-19C	179.7583	179.7595

41H-31C	1.0955	1.095505	42C-25C-21C	131.3788	131.3799	43C-42C-25C-21C	-179.332	-179.331
42C-25C	1.465304	1.465307	43C-42C-25C	109.0163	109.0165	44C-42C-25C-21C	1.048334	1.053557
43C-42C	1.415501	1.415472	44C-42C-25C	130.7687	130.7688	45C-43C-42C-25C	-179.301	-179.296
44C-42C	1.39265	1.392657	45C-43C-42C	119.4836	119.4846	46C-44C-42C-25C	179.3028	179.2972
45C-43C	1.391761	1.391764	46C-44C-42C	119.5028	119.5028	47H-44C-42C-25C	-0.51768	-0.52017
46C-44C	1.398936	1.398928	47H-44C-42C	120.798	120.7977	48C-46C-44C-42C	-0.10069	-0.10084
47H-44C	1.082862	1.082863	48C-46C-44C	121.5972	121.5976	49H-45C-43C-42C	-179.901	-179.906
48C-46C	1.404299	1.404303	49H-45C-43C	119.8	119.7988	50H-46C-44C-42C	-179.911	-179.909
49H-45C	1.078751	1.078753	50H-46C-44C	118.3193	118.3197	51C-43C-42C-25C	-0.25174	-0.25098
50H-46C	1.079315	1.079318	51C-43C-42C	110.5457	110.5481	52C-51C-43C-42C	-114.097	-114.095
51C-43C	1.541526	1.541534	52C-51C-43C	112.6903	112.6875	53C-51C-43C-42C	115.2437	115.2415
52C-51C	1.567722	1.567691	53C-51C-43C	113.9037	113.9065	54C-53C-51C-43C	47.08898	47.08604
53C-51C	1.570723	1.570752	54C-53C-51C	119.1503	119.145	55C-52C-51C-43C	-70.1896	-70.2168
54C-53C	1.537508	1.537529	55C-52C-51C	118.95	118.9567	56H-53C-51C-43C	-75.0715	-75.0736
55C-52C	1.535388	1.535442	56H-53C-51C	107.1135	107.1169	57H-53C-51C-43C	171.7268	171.7213
56H-53C	1.092877	1.092865	57H-53C-51C	107.0357	107.038	58H-52C-51C-43C	53.56349	53.53958
57H-53C	1.095313	1.095316	58H-52C-51C	106.9715	106.9708	59H-52C-51C-43C	166.8256	166.8016
58H-52C	1.093541	1.093551	59H-52C-51C	106.8615	106.8644	60C-48C-46C-44C	179.6972	179.7017
59H-52C	1.094727	1.094729	60C-48C-46C	122.5697	122.5696	61C-60C-48C-46C	-114.328	-114.331
60C-48C	1.547245	1.547233	61C-60C-48C	107.7562	107.7559	62C-61C-60C-48C	-179.198	-179.199
61C-60C	1.567089	1.567139	62C-61C-60C	116.5811	116.5812	63C-60C-48C-46C	6.107383	6.101796
62C-61C	1.537216	1.537199	63C-60C-48C	111.8393	111.8401	64C-60C-48C-46C	125.3826	125.379
63C-60C	1.54536	1.545353	64C-60C-48C	109.2207	109.2208	65C-27C-6C-1C	121.895	121.9189
64C-60C	1.55294	1.552921	65C-27C-6C	110.2347	110.2364	66C-27C-6C-1C	-0.27457	-0.24513
65C-27C	1.564465	1.564455	66C-27C-6C	112.4976	112.4962	67C-27C-6C-1C	-119.508	-119.48
66C-27C	1.545443	1.545441	67C-27C-6C	109.1479	109.1466	68C-65C-27C-6C	-60.1162	-60.1118
67C-27C	1.553434	1.553465	68C-65C-27C	115.8263	115.8262	69H-33C-31C-29C	59.69389	59.69316
68C-65C	1.535168	1.535183	69H-33C-31C	111.2982	111.2982	70H-32C-30C-29C	-177.261	-177.264
69H-33C	1.091131	1.091131	70H-32C-30C	109.6624	109.6621	71H-67C-27C-6C	60.04036	60.04263
70H-32C	1.092515	1.092515	71H-67C-27C	110.6635	110.6614	72H-67C-27C-6C	179.7955	179.7984
71H-67C	1.091682	1.091684	72H-67C-27C	110.2035	110.2027	73H-67C-27C-6C	-60.2749	-60.2721
72H-67C	1.092852	1.092855	73H-67C-27C	111.6504	111.6477	74H-66C-27C-6C	59.19033	59.18415
73H-67C	1.090729	1.090731	74H-66C-27C	112.5033	112.5	75H-66C-27C-6C	178.953	178.9465
74H-66C	1.090126	1.090136	75H-66C-27C	109.4159	109.415	76H-66C-27C-6C	-62.2389	-62.2458
75H-66C	1.092156	1.092171	76H-66C-27C	111.2522	111.2548	77H-65C-27C-6C	62.89049	62.89604
76H-66C	1.091684	1.091683	77H-65C-27C	108.5045	108.5083	78H-65C-27C-6C	177.1202	177.126
77H-65C	1.093811	1.093819	78H-65C-27C	107.4791	107.4785	79H-68C-65C-27C	57.83482	57.83758
78H-65C	1.095432	1.095443	79H-68C-65C	111.2918	111.291	80H-68C-65C-27C	177.531	177.5331
79H-68C	1.091214	1.091221	80H-68C-65C	110.417	110.4164	81H-68C-65C-27C	-62.9642	-62.9617
80H-68C	1.092293	1.0923	81H-68C-65C	111.9076	111.9078	82H-64C-60C-48C	-176.065	-176.067
81H-68C	1.091363	1.091367	82H-64C-60C	110.8938	110.8949	83H-64C-60C-48C	-56.6016	-56.6042
82H-64C	1.091162	1.091165	83H-64C-60C	110.2694	110.2697	84H-64C-60C-48C	63.53287	63.5292
83H-64C	1.091562	1.091567	84H-64C-60C	111.9054	111.9059	85H-63C-60C-48C	-64.2889	-64.2908
84H-64C	1.09093	1.09093	85H-63C-60C	111.8691	111.8687	86H-63C-60C-48C	56.97995	56.97782
85H-63C	1.091958	1.091959	86H-63C-60C	111.1738	111.1743	87H-63C-60C-48C	175.9161	175.9138
86H-63C	1.091568	1.091571	87H-63C-60C	110.2044	110.2044	88H-61C-60C-48C	-56.358	-56.3588
87H-63C	1.090084	1.090085	88H-61C-60C	108.2782	108.2764	89H-61C-60C-48C	57.80247	57.80089
88H-61C	1.093434	1.09343	89H-61C-60C	107.5387	107.5364	90H-62C-61C-60C	178.882	178.8743
89H-61C	1.094644	1.094642	90H-62C-61C	109.9222	109.9226	91H-62C-61C-60C	-61.8897	-61.8978
90H-62C	1.09237	1.092374	91H-62C-61C	112.1806	112.181	92H-62C-61C-60C	59.71401	59.70663
91H-62C	1.091051	1.091052	92H-62C-61C	111.9805	111.9815	93H-54C-53C-51C	57.61556	57.62472
92H-62C	1.091441	1.091443	93H-54C-53C	113.3164	113.3123	94H-55C-52C-51C	177.1394	177.1209
93H-54C	1.089192	1.089194	94H-55C-52C	109.3903	109.3846	95H-54C-53C-51C	177.2679	177.2885
94H-55C	1.092811	1.092799	95H-54C-53C	109.2533	109.2578	96H-55C-52C-51C	-64.0321	-64.0437
95H-54C	1.092881	1.092872	96H-55C-52C	112.2918	112.2865	97H-54C-53C-51C	-64.3902	-64.3691
96H-55C	1.090111	1.090089	97H-54C-53C	111.2634	111.2577	98H-55C-52C-51C	58.39063	58.37254
97H-54C	1.089863	1.089864	98H-55C-52C	112.1563	112.16			
98H-55C	1.089828	1.089811						

Table 2. Mulliken atomic charges of Exalite-392A by DFT/B3LYP/6-311G in vacuum and ethanol medium

No.	Atoms	Mulliken Charge		No.	Atoms	Mulliken Charge		No.	Atoms	Mulliken Charge	
		Vacuum	Ethanol			Vacuum	Ethanol			Vacuum	Ethanol
1	C	-0.14717	-0.22064	34	H	0.182606	0.177757	67	C	-0.68932	-0.47838
2	C	-0.0715	-0.04137	35	H	0.158814	0.183942	68	C	-0.43986	-0.52504
3	C	0.018452	-0.07184	36	H	0.177872	0.190988	69	H	0.222959	0.182198
4	C	-0.02637	0.013027	37	H	0.158345	0.181179	70	H	0.173079	0.17957
5	C	-0.18646	-0.16553	38	H	0.193009	0.182201	71	H	0.203606	0.177344
6	C	-0.05903	0.133239	39	H	0.15882	0.175922	72	H	0.169139	0.177518
7	H	0.158862	0.166585	40	H	0.279778	0.187978	73	H	0.248312	0.177179

8	H	0.162798	0.171674	41	H	0.257019	0.179963	74	H	0.244902	0.187104
9	H	0.318472	0.187501	42	C	-0.13401	-0.09331	75	H	0.150021	0.177612
10	C	-0.00799	-0.05194	43	C	-0.09883	0.03855	76	H	0.232744	0.184023
11	C	-0.08604	-0.06351	44	C	-0.02871	-0.0417	77	H	0.189201	0.176677
12	C	-0.0759	-0.11873	45	C	-0.19673	-0.16606	78	H	0.240205	0.174914
13	C	-0.13106	-0.182	46	C	-0.18955	-0.22065	79	H	0.199771	0.182234
14	H	0.159645	0.175503	47	H	0.158531	0.172414	80	H	0.170052	0.175376
15	C	-0.10097	-0.05551	48	C	0.16646	0.134822	81	H	0.17175	0.178513
16	H	0.153378	0.185808	49	H	0.192955	0.198814	82	H	0.175044	0.182185
17	H	0.159101	0.17148	50	H	0.147884	0.167586	83	H	0.185268	0.17861
18	C	0.122261	-0.0555	51	C	0.289883	-0.2976	84	H	0.161129	0.179644
19	C	-0.14038	-0.18123	52	C	-0.43591	-0.29527	85	H	0.176134	0.182303
20	C	-0.15154	-0.11494	53	C	-0.49492	-0.30332	86	H	0.184552	0.184524
21	C	-0.02895	-0.06313	54	C	-0.6773	-0.53797	87	H	0.173915	0.183301
22	H	0.154534	0.171465	55	C	-0.42968	-0.53433	88	H	0.17507	0.183755
23	C	-0.37078	-0.01936	56	H	0.106553	0.184038	89	H	0.179059	0.172582
24	H	0.213976	0.185878	57	H	0.23951	0.182596	90	H	0.173298	0.17788
25	C	-0.07368	-0.05609	58	H	0.231382	0.176736	91	H	0.181283	0.181412
26	H	0.161523	0.175675	59	H	0.262634	0.182656	92	H	0.178863	0.180728
27	C	0.216777	-0.22757	60	C	-0.27751	-0.21859	93	H	0.283546	0.181996
28	C	0.124026	-0.01853	61	C	-0.2906	-0.30519	94	H	0.162574	0.179352
29	C	-0.71132	-0.28777	62	C	-0.53252	-0.53446	95	H	0.2447	0.177826
30	C	-0.26204	-0.29344	63	C	-0.49878	-0.52558	96	H	0.143367	0.183724
31	C	-0.29918	-0.31228	64	C	-0.50074	-0.49338	97	H	0.161425	0.192413
32	C	-0.51983	-0.53612	65	C	-0.63849	-0.30476	98	H	0.197643	0.184827
33	C	-0.59415	-0.52018	66	C	-0.64069	-0.52052				

Table 3. Calculated thermodynamic parameters of Exalite-392A with DFT theory using B3LYP/6-311G basis set

Parameters	DFT/B3LYP/6-311G
Energy(kcal mol^{-1})	
Translational	0.889
Rotational	0.889
Vibrational	569.613
Total	571.390
Nuclear repulsion energy (Hartree's)	4946.83
Zero-point vibrational energy (kcal mol^{-1})	543.879
Entropy, S(Cal/Mol-Kelvin)	257.479
Molecular capacity of constant volume (cal mol^{-1} k^{-1})	
Translational	2.981
Rotational	2.981
Vibrational	166.830
Total	172.792
Rotational constants (GHz)	
A	0.23634
B	0.02202
C	0.02126
Rotational temperatures (Kelvin)	
A	0.01134
B	0.00106
C	0.00102

Table 4. Theoretical Excitation studies of Exalite -392A in vacuum and solvent medium using TDDFT/B3LYP/6-311G.

	Vacuum	Ethanol
Excitation energy (nm)	338.85	337.32
Oscillator strength	1.7481	1.7089

Table 5. HOMO and LUMO energy states values of Exalite – 392A in vacuum and ethanol medium

Molecular orbital	Energy in eV	
	Vacuum	**Ethanol**
LUMO+2	-0.3967	-0.6582
LUMO+1	-0.5975	-2.8470
LUMO	-1.3300	-2.8482
HOMO	-5.4563	-2.9915
HOMO-1	-6.1094	-2.9934
HOMO-2	-6.7372	-6.7273

Table 6. Physicochemical properties of Exalite – 392A with vacuum and solvents

Solvents	Energy band gap (E_g)	Ionization potential (I)	Electron affinity (A)	Electro negativity (χ)	Chemical hardness (η)	Chemical potential (μ)	Chemical Softness (s)	Global Electrophilicity (ω)
Vacuum	4.1263	5.4563	1.33	3.39315	2.06315	-3.39315	1.031575	11.87700464
Ethanol	0.1433	2.9915	2.8482	2.91985	0.07165	-2.91985	0.035825	0.305426898

5. References

1. J. Valenta, J. Dian, J. Hala, P. Gilliot, R. Le´vy, J. Chem. Phys. 111(1999) 9398.
2. Y. Zhao, E. de Beer, D.M. Neumark, J. Chem. Phys. 105 (1996) 2575.
3. Y. Zhao, E. de Beer, C. Xu, T. Taylor, D.M. Neumark, J. Chem. Phys. 105 (1996) 4905.
4. J. Remy, J. Nygard, A.P. Pasinski, D. Antoine, J. Chem. Phys. 105(1996) 1287.
5. L. Minyung, Bull. Korean Chem. Soc. 16 (1995) 126.
6. L. Shane, H. Greek, M.W. Georg Schulze, C.A. Blades, K.F. Haynes, R.F. Klein, B. Turner, App. Optics 37 (1998) 170.
7. M.I. Mazurenka, B.L. Fawcett, J.M.F. Elakas, D.E. Shallcross, A.J.Orr-Ewing, Chem. Phys. Lett. 367 (2003) 1.
8. Y.F. Nadaf, et. al., J. Mol. Str.(Theochem) 678 (2004) 177–181.
9. Lanke, Sandip K. and Nagaiyan Sekar. J. Fluorescence 26 (2016): 949-962.
10. Gaussview/Gaussian Guide and Exercise Manual, http://users.df.uba.ar/rboc/em3/GAUSSIAN_TRAIN.pdf
11. Becke, Axel D.. J. Chem. Phy. 98 (1993): 5648-5652.
12. Lee, Yang and Parr. Phy. rev. B, Condensed matter 37 2 (1988) 785-789 .
13. El-Daly, Samy A., Abdullah M. Asiri, Abdullah Y. Obeid, Salman Ahmad Khan, Khalid A. Alamry, Mahmoud A. Hussien and Abdullah G. Al-Sehemi. Optics and Laser Tech. 45 (2013) 605-612.
14. Ricci, Marilena, Cristiana Lofrumento, Emilio Mario Castellucci and Maurizio Becucci. Spectroscopy 2016 (2016) 1-10.
15. Alande, Balaji D., C G Renuka, G. N. Sushma, Mallya Suma, Basavaraja Sannakki and Y. F. Nadaf. (2019) 2100**,** 020110.
16. G.H. Pujar, M.N. Wari, B. Steffi, H. Varsha, et al. J. Mol. Liq 244 (2017) 453.
17. Hiremath, Seema S. Khemalapure, Subrat Kumar Pattanayak, Veerabhadrayya S. Negalurmath and Kotresh Obelannavar. J. Mol. Str. (2018): 362-374.
18. Foresman, James B.. J. American Chem. Soc. 123 (2001): 10142-10143.
19. Jalbout, Abraham F., Masoomeh Naseri, Mustapha Fazli, Heidar Raissi, Mahboobe Rezaei, Alireza Nowroozi and Aned de Leon. Int. J. Quantum Chem. 109 (2009): 1481-1496.
20. Renuka, C G, Y. F. Nadaf, G. Sriprakash and S Rajendra Prasad. J. Fluorescence 28 (2018): 839-854.
21. Khajuria, Yugal, Surbhi Sharma, Ujval Gupta, Satishwer Singh and Kamni. Mat. Focus 4 (2015): 338-345.
22. Zhang, Cai-Rong, Wanzhen Liang, Hongshan Chen, Yu-Hong Chen, Zhiqiang Wei and You-zhi Wu. J. Mol. Str.(theochem) 862 (2008): 98-104.
23. Matthews, Dennis B., Pierre P. Infelta and Michael Grätzel. Solar Energy Mat. and Solar Cells 44 (1996): 119-155.
24. Renuka, C G, Kalegowda Shivashankar, P. Boregowda, S. S. Bellad, M. V. Muregendrappa and Y. F. Nadaf. J. Soln. Chem. 46 (2017): 1535-1555.
25. Adamo, Carlo and Denis Jacquemin. Chem. Soc. Rev. 42 3 (2013): 845-56.
26. Babu, Numbury Surendra and Teshome Abute Lelisho. 3 6 (2012) 3916-3934.
27. Shivraj, B. Siddlingeshwar, Elena M. Kirilova, Sergey V. Belyakov, Darshan Devang Divakar and Abdulaziz Abdullah Alkheraif. Photochem. & photobio. Scie. : J. Euro. Photochem. Asso.and Euro. Soc.for Photobio. 17 4 (2018): 453-464.
28. Sushma, G. N., M. Suma, A.G. Pramod and Y. F. Nadaf. 2220 (2020) 130027.
29. Cheng, Ming, Xichuan Yang, Fuguo Zhang, Jianghua Zhao and Licheng Sun. J. Phy. Chem. C 117 (2013): 9076-9083.
30. Pramod, A.G., Y. F. Nadaf and C G Renuka. Spectrochimica acta. Part A, Mol.and biomol. Spectro. 223 (2019): 117288.